Radiation Physics and Chemistry 206 (2023) 110760

Contents lists available at ScienceDirect

Radiation Physics and Chemistry

journal homepage: www.elsevier.com/locate/radphyschem

Design of an X-ray irradiator based on a standard imaging X-ray tube with FLASH dose-rate capabilities for preclinical research

A. Espinosa-Rodriguez [a,1], A. Villa-Abaunza [a,1], N. Díaz [a], M. Pérez-Díaz [c], D. Sánchez-Parcerisa [a,b], J.M. Udías [a,b], P. Ibáñez [a,b,*]

[a] Nuclear Physics Group and IPARCOS, Department of Structure of Matter, Thermal Physics and Electronics, CEI Moncloa, Universidad Complutense de Madrid, Madrid, Spain
[b] Instituto de Investigación Sanitaria del Hospital Clínico San Carlos, Madrid, Spain
[c] Sedecal Molecular Imaging, Algete, Spain

ARTICLE INFO

Handling Editor: Dr. Chris Chantler

Keywords:
Irradiator
X-rays
FLASH
Preclinical research

ABSTRACT

We propose a new concept of small animal X-ray irradiator based on a conventional imaging X-ray tube for preclinical research. In this work we assessed its feasibility to deliver FLASH dose rates. Our design puts the imaging X-ray tube into a shielded cabinet, which makes the system affordable and suitable to use without disruption in existing laboratories and with minimum regulatory burden. Two conventional 150 kVp X-ray tubes were characterized with Gafchromic films for dose rates and dose uniformity. Monte Carlo simulations were also performed to model the irradiator, and the efficiencies of the tube and dose rates (with and without additional filtration) were calculated and compared with measurements. The feasibility of achieving ultra-high dose rates was determined from the rating charts provided by the manufacturer and measurements. The small animal irradiator proposed in this work was able to deliver conventional dose rate irradiation (0.5–1 Gy/min) at 150 kVp at 20 cm distance with minimum amount of filtration. FLASH irradiations (a 10 Gy dose delivered at >40 Gy/s) were also possible at the maximum capabilities of the tubes by placing the samples at the closest possible distances from the sources. A first prototype has already been built and characterized.

1. Introduction

The practice of radiation oncology has undergone a substantial improvement in all the stages of the radiotherapy process from treatment planning to delivery and verification, related to the huge technological advances introduced during the last decades. However, the progress in our understanding of radiobiological processes has fallen behind (Syme et al., 2009). Take for instance FLASH therapy, meaning the delivery of a substantial dose fraction at ultra-high dose rates (UHDR) (Favaudon et al., 2014; Wilson et al., 2020). FLASH irradiation significantly reduces normal tissue toxicity compared to conventional radiotherapy, while maintaining tumor control probability at a similar level (Favaudon et al., 2014; Zhang et al., 2020; Mazal et al., 2020). The standard dose rate used in conventional radiotherapy (electrons and photons) and proton therapy is around a few cGy/s, so a typical therapeutic dose-fraction of 2 Gy may be delivered in several seconds or minutes. But a study in 2014 (Favaudon et al., 2014) demonstrated a drastic reduction in lung fibrosis in mice irradiated with electron beams at UHDR (≥40 Gy/s), while exhibiting similar effectivity to conventional dose rate radiotherapy in the suppression of tumor growth. Several experiments have been performed since then in other animals, such as zebrafish, mice, cats and mini-pigs (Fouillade et al., 2020; Montay-Gruel et al., 2018; Vozenin et al., 2019) at FLASH rates with similar findings. In 2018, the first patient was treated with FLASH radiotherapy (Bourhis et al., 2019). The FLASH effect has been observed independently by different groups using protons (Beyreuther et al., 2019), X-rays (Montay-Gruel et al., 2018) and electrons (Schüler et al., 2017), but its underlying biological mechanisms still remain unknown (Mazal et al., 2020). Furthermore, there are several physical beam parameters (instantaneous dose rate, total dose, duty cycle or treatment time) which may impact the biological response of the irradiation (Friedl et al., 2022; Vozenin et al., 2020; Espinosa-Rodriguez et al.,

* Corresponding author. Nuclear Physics Group and IPARCOS, Department of Structure of Matter, Thermal Physics and Electronics, CEI Moncloa, Universidad Complutense de Madrid, Madrid, Spain.
E-mail address: pbibanez@ucm.es (P. Ibáñez).
[1] The first two authors of this work have made equal contributions to the manuscript and the associated scientific research.

https://doi.org/10.1016/j.radphyschem.2023.110760
Received 20 July 2022; Received in revised form 11 November 2022; Accepted 2 January 2023
Available online 3 January 2023

2022). An improvement of the accuracy, availability and reproducibility of radiobiology experiments at both conventional and FLASH conditions, would greatly help to fill this gap. This motivates the development of advanced radiation systems to perform experiments, in animal and in cell cultures, able to reproduce clinically relevant radiation exposure conditions (Kuess et al., 2014; Ghita et al., 2019), at conventional and ultra-high dose rates. However, experiments at UHDR suffer from limited availability of capable treatment machines. For example, standard clinical LINACS must be non-trivially tweaked to produce FLASH dose rates (Felici et al., 2020; Rahman et al., 2021; Lempart et al., 2019). The higher cost and even lower availability of powerful enough radiation sources, such as synchrotrons or cyclotrons, also precludes their use. On the other hand, X-ray irradiators for preclinical research are becoming increasingly popular in cancer research and specially in radiobiology experiments (Ghita et al., 2019), representing an alternative to traditional gamma irradiators with several advantages, such as their relative low cost, ease of use, smaller certification/authorization burden, less safety concerns and good control of dose rate. Therefore, a FLASH capable X-ray irradiator would be of interest.

Some previous work has been done regarding the capability of delivering UHDR with X-ray tubes (Esplen et al., 2020). Bazalova-Carter and Esplen (Bazalova-Carter and Esplen, 2019) evaluated the maximum dose rates achievable with two X-ray tubes with a beryllium window and stationary anode with half-value layers (HVL) of 87 μm and 78 μm aluminum scored just below the window, and obtained dose rates >100 Gy/s at about 3.5 cm from the focal spot at 160 kVp. FLASH dose regions were obtained with depths up to 2 mm for a 1 cm diameter area, which was suitable for *in vitro* FLASH experiments. More recently, Cecchi et al. (2021) developed an X-ray beam shutter system with a sample holder for one of the previously studied X-ray tubes, enabling <1 s irradiations at ultra-high dose rates. When rotating anode X-ray tubes are used, the heat loading capacity increases by two orders of magnitude, so Rezaee et al. (2021) proposed an irradiator with two parallel-opposed 150 kV X-ray sources of the kind employed in fluoroscopy, with a rotating anode, and estimated a capability of delivering 10–50 Gy doses at dose rates of 40–200 Gy/s with depth-dose uniformity and field dimensions that are sufficient for the irradiation of murine models. Two X-ray sources, with nominal powers above 110 kW, were proposed for the study.

In this work, we designed a small animal X-ray irradiator using a conventional X-ray head for imaging and studied its feasibility of delivering FLASH dose rates. The choice of a conventional X-ray source was motivated by the low price, high availability and wide variety of models in the market. In contrast, X-ray tubes specifically designed for irradiations are more expensive and there are much fewer models available (Verhaegen et al., 2011; Biglin et al., 2019). Our study included the characterization of two X-ray tubes with radiochromic films and their modeling with Monte Carlo (MC). The proposed system included a commercial X-ray source with planar emission and a tube voltage up to 150 kV, with a standard continuous wave, high voltage electronic generator, the same one employed in current chest X-rays. The prototype was built by SEDECAL (Sociedad Española de Electromedicina y Calidad, S.A), one of the largest manufacturers of X-ray portable imaging systems worldwide.

2. Materials and methods

2.1. General considerations of the irradiator

The irradiator consisted of a fixed X-ray tube located inside a shielded box with a movable platform. Design' requirements were:

- Compact size, modest shielding requirement, minimal certification burden.
- Very competitive price, based upon conventional X-ray heads and high voltage generators, which, due to its high standardization and the involvement of SEDECAL, were readily available and at very interesting prices.
- Simple operation, user-friendly and accurate. Able to irradiate several mice in less than 15 min.
- Potential to achieve ultra-high dose rates, above 40 Gy/s (FLASH-RT), while delivering 6–10 Gy fractions, to in-vitro targets, such as Petri dishes with cell cultures, in a single shot, with irradiation times limited to few milliseconds (Wilson et al., 2020; Montay-Gruel et al., 2018).

Table 1
Specifications of the Toshiba E7252X and E7869X X-ray sources.

	E7252X	E7869X
Max Voltage (kVp)	150	150
Focal Spot size (mm)	0.6, 1.2	0.6, 1.3
Anode angle (deg.)	12	12
Anode diameter (mm)	74	100
Nominal anode input power (at 0.1 s)	75 kW	100 kW
Inherent filtration	0.9 mm Al	1.1 mm Al
External filtration (mm)	–	1 mm Al+0.1 mm Cu/ 1 mm Al+0.2 mm Cu/ 2 mm Al
Target	Re-W-Mo	Re-W-Mo
X-ray coverage at 1000 mm (mm)	430 × 430	430 × 430
Distance from focal spot to exit window (mm)	53	60
Generator	SHFR300-TF400 (30 kW)	SHFR300-TF400 (30 kW)

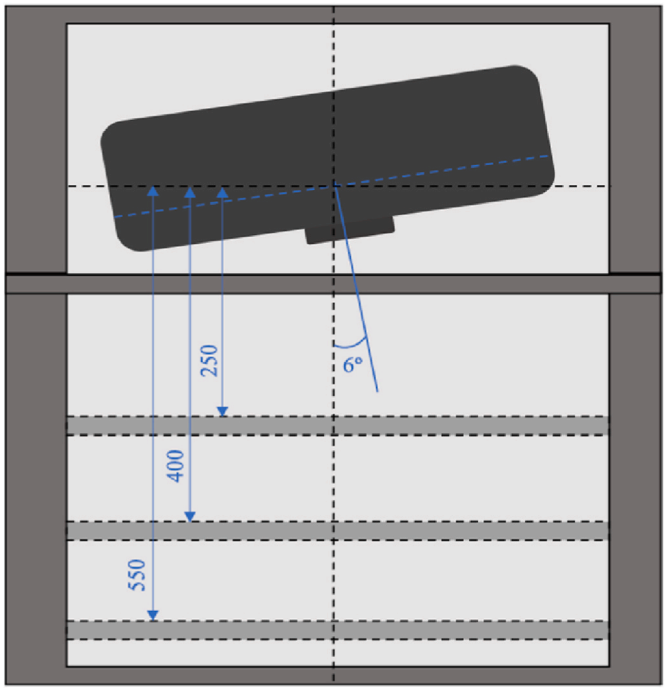

Fig. 1. Simplified scheme of the irradiator built by SEDECAL.

We focused on two very common rotating anode X-ray heads from Toshiba, models E7869X (Toshiba E7869X PI) and E7252X (Toshiba E7252X PI). Table 1 summarizes the main characteristics of these tubes. They were coupled to a high frequency, high efficiency, continuous wave, solid-state high voltage SHFR300 generator for X-ray systems manufactured by SEDECAL (SEDECAL webpage).

Both sources could produce beams with either small (0.6 mm) or

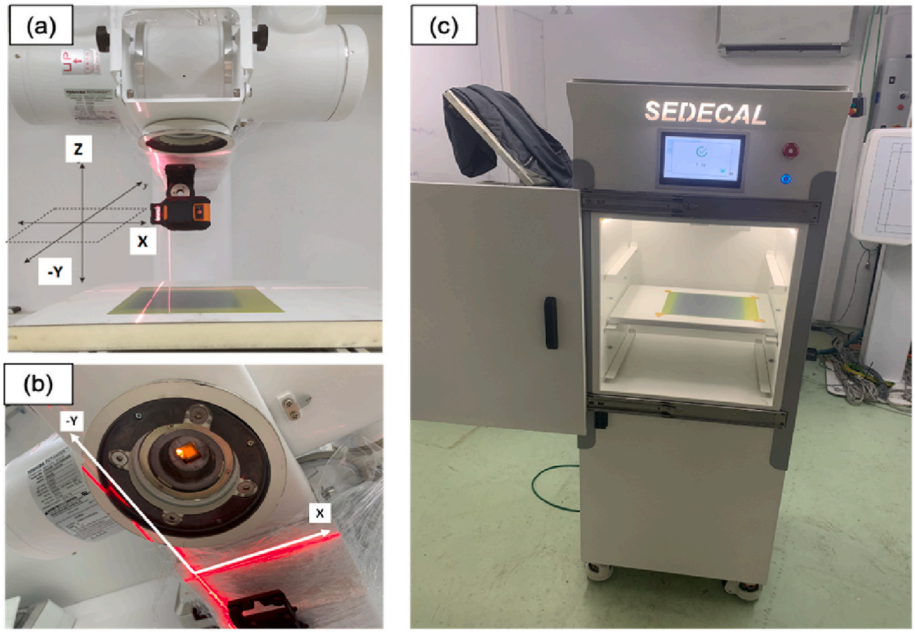

Fig. 2. (a) and (b) Laser mounted in the X-ray head to mark the position and the center of coordinates during the first set of measurements. (c) Picture from the second set of measurements with the film placed inside the prototype of the irradiator.

large (1.2 mm) focal spots. In order to maximize the dose rate, the large focal spot was used in all the measurements and calculations (Senda et al., 2004). The anodes were made of a molybdenum body with a tungsten-rhenium surface and a target angle of 12°, so they provided equal radiation coverage. Inherent tube filtrations were made of aluminum and the thickness ranged between 0.9 and 1.1 mm. Additionally, Toshiba E7869X was mounted on a head which allowed for selecting several external filter combinations. The maximum nominal X-ray tube potential was limited to 150 kVp.

The generator employed in this work was limited to 30 kW maximum continuous power, while the anode was kept spinning at maximum rotation speed, fed from a specialized output power connector of the high voltage generator, controlled by firmware independently of the high voltage supply.

A prototype of the irradiator was built by SEDECAL. It incorporated the Toshiba E7252X tube with a SHFR300 generator (30 kW) placed in a lead box with a movable platform that could be positioned at three distances from the source: 25, 40 and 55 cm. The tube was tilted 6° to try to decrease the heel effect. The user can choose the dose and the position of the platform in a screen located outside the box. A scheme of the device is shown in Fig. 1. Shieldings and locks were designed to allow the irradiator to be operated in a non-controlled area.

2.2. Measurements

EBT2 and EBT3 Gafchromic films (Ashland Advanced Materials, NJ, USA) were used to perform a dosimetric characterization of the Toshiba E7252X and E7869X X-ray tubes. Gafchromic films provide better spatial resolution than array devices, wide dose ranges and energy-independent dose response (Niroomand-Rad et al., 1998). A calibration curve was made with EBT3 films from the same batch at different dose levels from 0.5 Gy to 12 Gy with a 6-MV beam in a Siemens Artiste linear accelerator (Munich, Germany) (Sanchez-Parcerisa et al., 2021). All films were scanned using an Epson Perfection V850 flatbed scanner with 150 ppi and 48-bit raw image resolution. Scans were performed at least 24 h post irradiation. The scanning protocol described by Avanzo et al. was adopted (Avanzo et al., 2012). Film images were analyzed using an in-house image manipulation routine written with MATLAB 7.6.0.324 (MathWorks, Natick, MA, USA) based on the three-channel technique (Micke et al., 2011).

2.2.1. Dosimetric characterization of the X-ray tubes

Irradiation of several EBT3 films was performed at several distances, current and voltage to measure the delivered dose of the tubes. External filtration was used when possible. Films were cut into 4 × 7 cm^2 pieces, and they were placed between two 2-mm thick PMMA layers to avoid

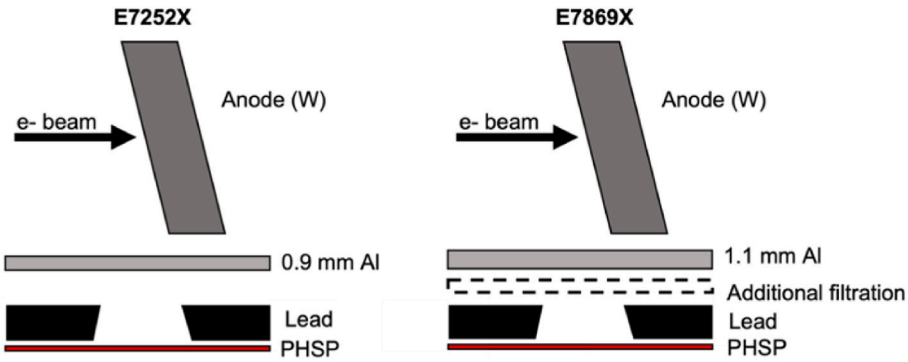

Fig. 3. Scheme of the geometries simulated with TOPAS for both X-ray tubes.

Table 2
Experimental dose with radiochromic films for both tubes measured at 150 kV.

Tube	Additional Filtration	Voltage (kV)	Intensity (mA)	Power (W)	Time (s)	Distance (cm)	Dose (Gy)	Dose Rate Films (Gy/s)
Toshiba E7252X	No	150	200	30,000	0.5	6.0	7.30 ± 0.29	**14.60 ± 0.58**
		150	200	30,000	4.8	24.0	6.53 ± 0.26	**1.02 ± 0.04**
		150	200	30,000	10.0	32.0	6.50 ± 0.26	**0.56 ± 0.02**
Toshiba E7869X	No	150	160	24,000	4.0	32.6	1.58 ± 0.06	**0.40 ± 0.02**
	1 mm Al + 0.1 mm Cu	150	125	18,750	4.0	32.6	0.97 ± 0.04	**0.24 ± 0.01**
	1 mm Al + 0.2 mm Cu	150	125	18,750	5.0	32.6	0.80 ± 0.03	**0.16 ± 0.01**
	2 mm Al	150	100	15,000	6.3	32.6	1.18 ± 0.05	**0.19 ± 0.01**

buildup and reduce backscatter. Beam intensity was limited by the maximum input power allowed by the high voltage generator in continuous irradiation.

The possibility of achieving ultra-high dose rates beyond the FLASH threshold in a single shot was also studied. For this measurement, the E7252X tube operation voltage was fixed at 150 kV and a film was positioned at 6 cm from the source.

2.2.2. Uniformity of the dose

Two sets of dose measurements were performed to determine the uniformity of the dose in the irradiated areas with the E7252X tube. The first one was performed with the detached tube placed perpendicular to the films (Fig. 2a). The second set was directly made with the prototype of the irradiator with the film placed inside the lead box (Fig. 2c). Films were cut into pieces of approximately 20 × 20 cm^2 and were placed at different distances from the Toshiba E7252X tube. A small crosshair laser was mounted on the head of the irradiator, pointing towards the radiochromic, to mark the position in each film before irradiation.

2.3. MC simulations

Toshiba E7252X and E7869X X-ray sources were modeled with TOPAS version 3.0.1, using the default physics list (Perl et al., 2012). Previous works supported the capability of the TOPAS-MC tool to perform simulations of X-rays (Cecchi et al., 2021; Hewson et al., 2018; Sotiropoulos et al., 2021; Lu et al., 2017). The simulations were based on tube parameters listed in Table 1, with and without additional filtration, for different tube voltages.

Fig. 3 shows a simplified scheme of the geometry considered for the MC calculations. The tungsten–rhenium alloy was replaced by a 100% tungsten anode, because the effect of this change on the generated radiation is negligible (Rezaee et al., 2021). Monoenergetic electron beams with 10^{10} particles and energies from 50 keV to 150 keV were simulated impinging in the lowest edge of the tungsten target. The emerging X-rays were collected in a phase-space (PHSP) file placed after the exit window. Energy spectra were extracted, and efficiency (ε) was calculated as the ratio between the number of X-rays reaching the PHSP (N_x) and the original number of electrons (N_e).

$$\varepsilon(\%) = \frac{N_x}{N_e} 100 \tag{1}$$

The PHSP files were used for the calculation of dose deposition in a PMMA phantom with 1.0 × 1.0 × 0.5 mm^3 voxels located at different distances from the focal spot and 10^8 histories, in order to reproduce the experimental measurements. Dose rates ($\overline{D}$) were calculated following the approach described by Bazalova-Carter and Esplen (Bazalova-Carter and Esplen, 2019) and Rezaee et al. (2021):

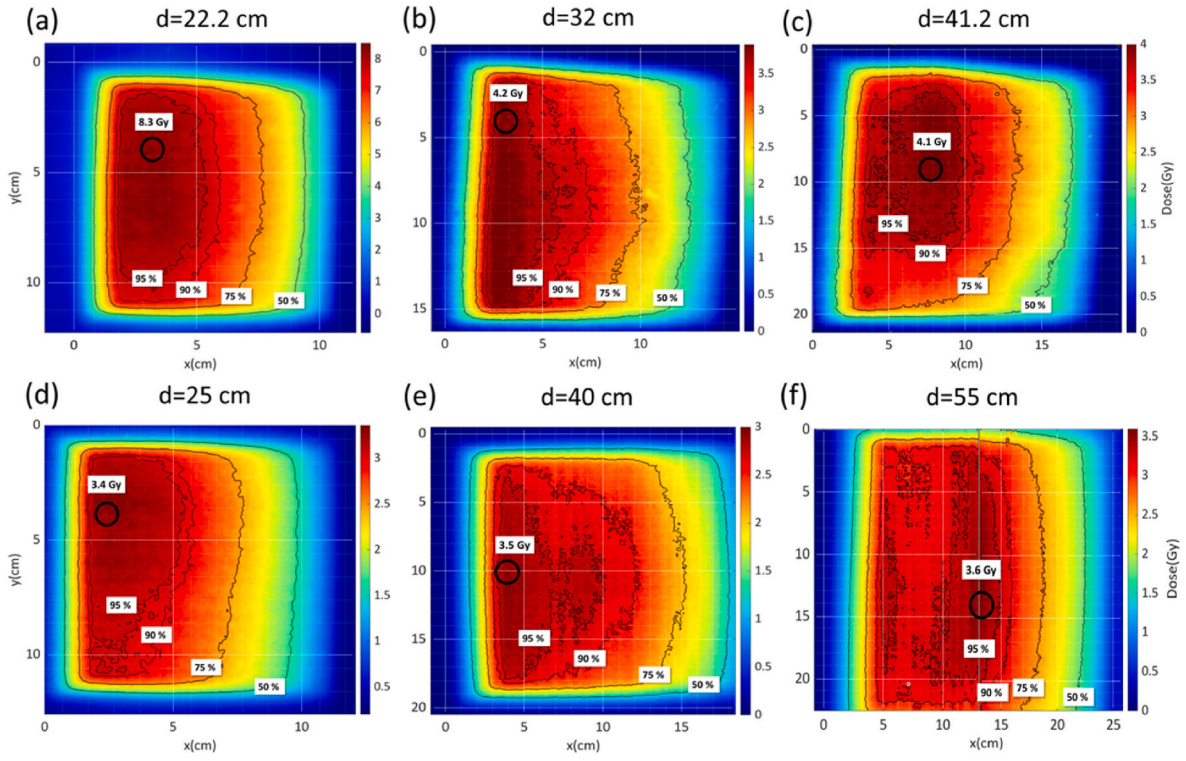

Fig. 4. 2D dose maps and isodose contours from the radiochromic films. The first row corresponds to the set of measurements taken with the bare tube perpendicular to the films. The second row corresponds to the set of images taken with the films placed inside the irradiator.

Table 3
95% and 90% of the maximum dose isodose regions obtained from all the films irradiated in the two sets of measurements.

# Set of measurements	# Film	Distance (cm)	95% isodose region (cm^2)	90% isodose region (cm^2)
Tube placed directly on sample	A	22.4	3.0 × 9.0	4.0 × 10.0
	B	32.0	3.0 × 13.0	4.0 × 13.0
	C	41.2	5.0 × 10.0	7.0 × 12.0
Tube mounted on the irradiator	D	25.0	3.0 × 7.0	4 × 9.5
	E	40.0	2.5 × 13.0	8.0 × 13.0
	F	55.0	4.0 × 18.0	11.0 × 20.0

$$\overline{D} = \frac{D \cdot I \cdot \varepsilon}{N_x \cdot Q \cdot 100} \quad (2)$$

Where D is the MC dose in Gy, I the intensity and Q the electron charge ($1.602 \cdot 10^{-19}$ C).

Half-value layers (HVLs) of the X-ray beams were calculated from the simulated spectra extracted from the PHSP at the surface of both X-ray tubes (with and without additional filtration) using the methodology described by Verhaegen et al. (1999).

2.4. Feasibility of FLASH irradiations

Based on the measurements performed with the Toshiba E7252X and E7869X tubes, we estimated the feasibility to perform FLASH irradiation experiments. Dose rates per mAs were calculated from the measurements at the minimum possible distance from the source (ie., the exit window) which was 5.3 cm for E7252X and 6 cm for E7869X. These values were used, in combination with data from the rating charts provided by the manufacturers, to calculate dose rates for dose deliveries between 6 and 10 Gy with the shortest possible irradiation times.

3. Results

3.1. Dosimetric characterization

Dosimetric characterization was done for both tubes at different distances, voltages and intensities. The results obtained at 150 kV are presented in Table 2. At 6 cm from the source, a dose rate of 14.6 Gy/s was achieved with the E7869X tube. At 20 cm from the source, dose rates higher than 1 Gy/min were achieved without additional filtration and with the tubes at their maximum capacity. If additional filtration was considered, dose rates decreased significantly by more than 20% up to 50%. A 4% uncertainty was estimated for the dose obtained from the EBT3 films, which takes into account every possible source of uncertainty according to the AAPM recommendations (reference beam calibration, uniformity, distance and film position, scanner properties, etc.) (Niroomand-Rad et al., 1998). The associated uncertainties in the intensities, voltages and irradiation times defined in the fully electronic generator were much smaller, thus they were neglected.

3.2. Dose uniformity

Fig. 4 shows 2D dose maps acquired at different distances from the X-ray head for the two sets of measurements. The first row corresponds to

Table 4
Calculated HVLs at 150 kV obtained at the exit of the X-ray tubes.

Tube	Additional Filtration	HVL (mm Al)
Toshiba E7252X	No	3.7
Toshiba E7869X	No	4.1
	1 mm Al + 0.1 mm Cu	7.2
	1 mm Al + 0.2 mm Cu	8.6
	2 mm Al	5.7

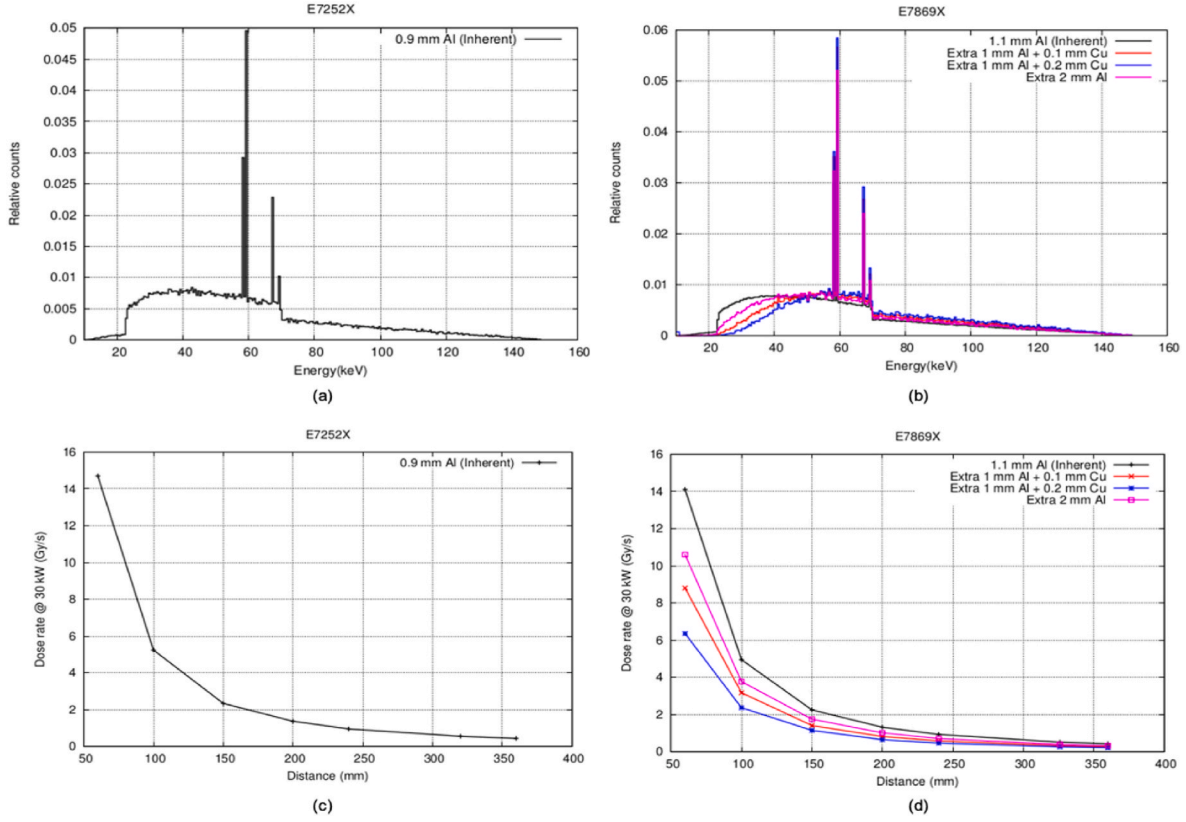

Fig. 5. Simulated energy spectra of the 150 kVp X-ray beam for the Toshiba E7252X (a) and the Toshiba E7869X (b) tubes, with and without additional filtration, and their corresponding simulated dose rates ((c) and (d)) considering a 30-kW generator at different distances.

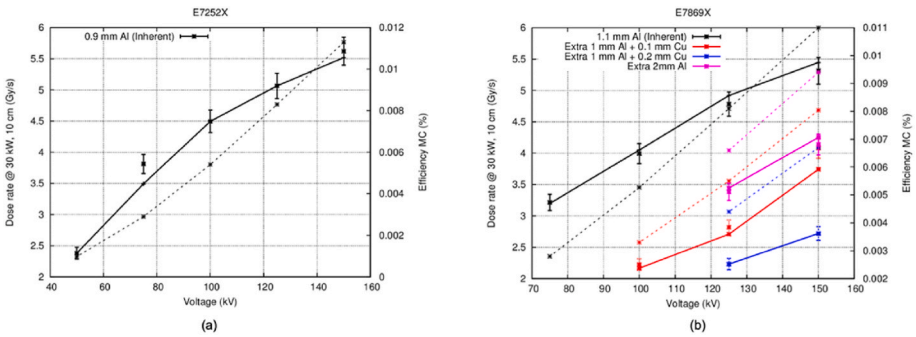

Fig. 6. Comparison of dose rates at 30 kW and 10 cm distance derived from measurements (points) and MC simulations (solid lines) at different voltages, with and without additional filtration, for the E7252X tube (a) and with the E7869X tube (b). Measurements and simulations are in very good agreement. The tube efficiencies derived from the MC simulations (dashed lines, right axis of the figure) are also plotted.

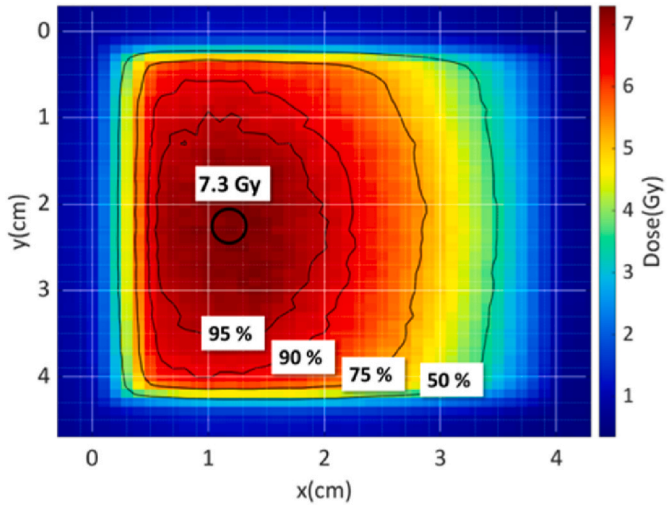

Fig. 7. 2D dose map from the FLASH irradiation including the isocontours of the 95%, 90%, 75% and 50% regions.

the first set of measurements with the spared tube perpendicular to the films and the second row corresponds to the set of measurements with the films placed inside the irradiator. The 95%, 90%, 75% and 50% isodose regions of the maximum dose are included, as well as the maximum dose. Table 3 summarizes the sizes of 95% and 90% isodose regions. At the tray located at the shortest distance from the source, the 95% isodose area is 3.0 × 7.0 cm^2, which is already large enough for preclinical research with small animals or cell cultures.

3.3. MC simulations

The energy spectra for 150 kVp X-ray beams obtained from the MC simulations of both tubes are shown in Fig. 5 (a) and (b), and the simulated dose rates obtained from these spectra at different distances from the source after 2 mm of PMMA for a 30-kW generator are presented in Fig. 5 (c) and (d). The inherent filtration of the E7869X was 1.1 mm Al, while for the E7252X it was 0.9 mm Al. Consequently, the X-ray beam from the E7869X was slightly more hardened and the dose rate was lower than the one from the E7252X. When additional external filtrations were considered, dose rates decreased around 25% for the 2 mm Al filter, 35% for the 1 mm Al + 0.1 mm Cu filter and up to 50% for the 1 mm + 0.2 mm Cu filter. Beam hardening can also be appreciated in Table 4, which includes the calculated HVLs (in mm Al) at the exit of the X-ray tubes obtained for all filtrations.

Fig. 6 includes a comparison of measured (points) and simulated (solid lines) dose rates at 30 kW and 10 cm distance with both tubes at different working voltages, as well as the efficiencies obtained from the MC simulations (dashed lines, right axis of the figure), with and without additional filtration. The simulations accurately reproduced the experimental data, with relative dose differences well below 5% in most cases.

3.4. Feasibility of FLASH irradiations

Fig. 7 shows the 2D map corresponding to the FLASH irradiation at 6 cm with the Toshiba E7252X tube. The maximum dose measured was 7.3 Gy, delivered at 14.6 Gy/s. Within the 95% isodose region, a minimum dose rate of 13.1 Gy/s can be achieved in a field size of 14 × 22 mm^2. Dose rate was limited to 30 kW of continuous DC power, due to the firmware of the generator. Duration of the irradiations can be set with 1 ms accuracy, as the DC generator can switch on and off several thousands of times per second. The time, charge and voltage delivered to the X-ray source is actively monitored by the generator electronics. We have verified that the repeatability of the doses delivered by very short pulses is better than the accuracy estimated for the dose measurements of 4%. If the maximum intensity values from the tube's rating charts were used, FLASH dose rates above 40 Gy/s could be achieved for both tubes at the exit window, as it is presented in Table 5, which includes the dose rates calculated for the Toshiba E7252X and the Toshiba E7869X at 5.3 cm and 6 cm, respectively, for integrated doses between 6 and 10 Gy. Uncertainties of the dose rates were estimated as 15% to take into account, besides the 4% uncertainty associated to the dose measurement, differences that may appear between the data from the manufacturer's tables for a generic model of each tube and the specific tubes we worked with.

Table 5
Dose rates calculated for doses delivered between 6 and 10 Gy at the minimum distance, with the shortest possible irradiation times for the Toshiba E7252X and the Toshiba E7869X.

Toshiba E7252X					Toshiba E7869X				
Distance (mm)	Total Dose (Gy)	Dose Rate (Gy/s)	Irradiation time (s)	Power (kW)	Distance (mm)	Total Dose (Gy)	Dose Rate (Gy/s)	Irradiation time (s)	Power (kW)
53	6	44.6 ± 6.7	0.12	71.5	60	6	45.6 ± 6.8	0.13	96.4
	7	43.4 ± 6.5	0.15	69.7		7	44.7 ± 6.7	0.15	94.5
	8	42.1 ± 6.3	0.17	67.5		8	43.4 ± 6.5	0.17	91.7
	9	41.0 ± 6.2	0.20	65.7		9	42.4 ± 6.4	0.19	89.5
	10	39.7 ± 6.0	0.22	63.5		10	41.3 ± 6.2	0.22	87.3

4. Discussion and conclusions

In this work we have proposed a design for a small animal X-ray irradiator to be used in preclinical research. We used a conventional X-ray tube for imaging and a shielded cabinet, which made the system affordable and suitable to use without disruption in existing laboratories.

A dosimetric characterization of conventional X-ray tubes up to 150 kVp was performed, and measurements with radiochromic films proved that both tubes without additional filtration were able to deliver dose rates of 0.5–1 Gy/min at 20–25 cm from the source, as requested for conventional preclinical irradiations (typical small animal doses range between 2 and 10 Gy while being delivered in 1–10 min) (Yoshizumi et al., 2011), and D90 isodose regions at that distances were big enough to fit 3–4 mice. An optimal pattern of irradiation, in terms of the time required to achieve the total dose avoiding thermal overcharge of the tube and/or the generator, consisted in administering pulses of 200 mA for about a second, separated by a 10 s interval. Pulsed operation further allowed to run SEDECAL high voltage generators from batteries or super-capacitors or a combination of both, that the company develops to be used in mobile X-ray imaging equipment. The use of energy storage units also simplifies the requirements of the AC plug to be employed for the system, as a single phase 220 AC, 5 kW supply would be enough to operate the irradiator.

There is growing interest in performing FLASH preclinical research with conventional X-ray tubes, which overcomes the current limitations of the accelerator technologies used in this field. Bazalova-Carter et al. (Bazalova-Carter and Esplen, 2019) evaluated the possibility of delivering FLASH dose rates with two industrial 160 kVp X-ray tubes with stationary anode and were able to deliver up to 160 Gy/s at 3.5 cm from the anode in 30 s irradiations. Shorter irradiations were not possible due to the tube ramp-up and cool-down times. Recently, they have developed a custom X-ray beam shutter to enable the delivery of < 1s irradiations (Cecchi et al., 2021). This system would provide ultra-high dose rates up to around 110 Gy/s for samples smaller than 0.3 mm. Rezaee *et at* (Rezaee et al., 2021). proposed an ultra-high dose rate irradiator composed of two 150 kVp fluoroscopy X-ray sources in a parallel-opposed arrangement to obtain a uniform dose rate in the central region of a 2 cm phantom with dose rates from 180 Gy/s at the surface to 140 Gy/s at the center. However, despite the promising results, the system would be complex and quite expensive.

To check the feasibility of delivering FLASH dose rates with our system, measurements were performed to assess the maximum dose rate the E7252X system could deliver, as well as its ability and repeatability of administering very short pulses, thanks to the modern design of the DC generator. A radiochromic film was placed at 6 cm from the anode and the maximum voltage and intensity were selected. Integral, single shot doses in excess of 7 Gy at dose rates of 14.6 Gy/s were achieved. This result is comparable with the measurement obtained by Rezaee et al. of 20 Gy/s at 6.6 cm with a 150 kVp X-ray tube and a 0.5 mm Al inherent filter for the same input power of 30 kW (Rezaee et al., 2021). There is some consensus that single doses of >8 Gy delivered at rates above 40 Gy/s, are clearly within the FLASH regime, after the work of Favaudon et al. (2014), while the onset of protective effect may show up at average dose rates well below 10 Gy/s (Montay-Gruel et al., 2019). Labarbe et al. (2020) performed a series of simulations to estimate the normal tissue complication probability (NTCP) as a function of the average dose rate using some available experimental data. Their results suggested a critical region, between 10 and 100 Gy/s, in which the NTCP could be gradually reduced as the dose rate was increased and remained low for higher dose rates. The dose rate that we obtained with the E7252X would be in this region.

The acquisitions with the Toshiba E7252X were limited by the firmware of the high voltage generator employed, well below the peak power capacity of the X-ray tubes employed. From the rating charts from the manufacturer, we estimated that doses of 10 Gy in a single shot could be delivered at dose rates of 40 Gy/s at the exit windows of either the E7252X or E7869X, deep within the FLASH region. A new prototype is being developed based on a 50-kW high voltage generator from SEDECAL which combines energy storage capabilities with a custom SEDECAL development for the X-ray tube and generator assembly, which will allow to have the exit window at less than 3 cm from the focal spot and would reach dose rates well above 100 Gy/s.

In a modern electronic DC-HV generator such as the one employed in this work it is possible to monitor the actual time and intensity delivered to the X-ray source several thousand times per second. The software + firmware of the generator allows setting the irradiation time, in ms steps, as well as the intensity. The integrated charge delivered by the generator to the X-ray tube can also be completely monitorized. We have verified the repeatability of the dose delivered per pulse, for pulses down to a fraction of a second and found them to be excellent, with deviations below the accuracy of the radiochromic film or ionization chamber employed to verify the dose. With regards to FLASH rates, short irradiations do not pose a problem, as the DC voltage can be changed and even switched on or off within less than 1 ms time lapse. Long irradiations, on the other hand, to obtain >10 Gy doses at conventional rates and relatively large areas with continuous irradiations pose more of a problem, due to the thermal budget in the generator and the X-ray tube. Electronic protections are in place to protect the generator and the tube from over-heating.

It can be concluded that X-ray irradiators designed along the lines described in this work would meet all the requirements stated in the introduction. The reduced dimensions of the device resulting from minimal shielding requirements and the use of a conventional X-ray tube result in an unquestionable cost-effectiveness. Additionally, its operation is very user friendly: the user is required to enter the intended dose value in a screen and the system calculates the beam parameters related to such dose. But the most attractive characteristic is, probably, the suitability for both conventional irradiations, being able to irradiate a few mice (3–4) in less than 15 min, and FLASH irradiations, with the potential to achieve ultra-high dose rates over 40 Gy/s while delivering a total dose of 6–10 Gy in the target, such as Petri dishes with cell cultures, in a single shot, with irradiation times limited to few milliseconds.

Declaration of competing interest

The authors declare the following financial interests/personal relationships which may be considered as potential competing interests: M. Perez-Diaz reports a relationship with SEDECAL Medical Imaging that includes: employment.

Data availability

No data was used for the research described in the article.

Acknowledgments

This work was funded by Comunidad de Madrid under project B2017/BMD-3888 PRONTO-CM “Protontherapy and nuclear techniques for oncology”. Support by the Spanish Government (RTI 2018-098868-B-I00, RTC-2015-3772-1, XPHASE-LASER, CPP 2021-008751 NEW-MBI), as well as European Regional and Resilience Funds, and the European Union’s Horizon 2020 research and innovation programme under the Marie Sklodowska-Curie grant agreement No 793576 (CAPPERAM) is acknowledged.

This is a contribution for the Moncloa Campus of International Excellence, “Grupo de Física Nuclear-UCM”, Ref. 910059. Part of the calculations of this work were performed in the “Clúster de Cálculo para Técnicas Físicas”, funded in part by UCM and in part by EU Regional Funds.

References

Avanzo, M., Rink, A., Dassie, A., Massarut, S., Roncadin, M., Borsatti, E., Capra, E., 2012. In vivo dosimetry with radiochromic films in low-voltage intraoperative radiotherapy of the breast. Med. Phys. 39 (5), 2359–2368.

Bazalova-Carter, M., Esplen, N., 2019. On the capabilities of conventional x-ray tubes to deliver ultra-high (FLASH) dose rates. Med. Phys. 46 (12), 5690–5695.

Beyreuther, E., Brand, M., Hans, S., Hideghéty, K., Karsch, L., Leßmann, E., Schürer, M., Szabó, E.R., Pawelke, J., 2019. Feasibility of proton FLASH effect tested by zebrafish embryo irradiation. Radiother. Oncol. 139, 46–50.

Biglin, E.R., Price, G.J., Chadwick, A.L., Aitkenhead, A.H., Williams, K.J., Kirkby, K.J., 2019. Preclinical dosimetry: exploring the use of small animal phantoms. Radiat. Oncol. 14 (1), 1–10.

Bourhis, J., Sozzi, W.J., Jorge, P.G., Gaide, O., Bailat, C., Duclos, F., Patin, D., Ozsahin, M., Bochud, F., Germond, J.-F., 2019. Treatment of a first patient with FLASH-radiotherapy. Radiother. Oncol. 139, 18–22.

Cecchi, D.D., Therriault-Proulx, F., Lambert-Girard, S., Hart, A., Macdonald, A., Pfleger, M., Lenckowski, M., Bazalova-Carter, M., 2021. Characterization of an x-ray tube-based ultrahigh dose-rate system for in vitro irradiations. Med. Phys. 48 (11), 7399–7409.

Espinosa-Rodriguez, A., Sanchez-Parcerisa, D., Ibáñez, P., Mazal, A., Vera Sanchez, J.A., Fraile, L.M., Udias, J.M., 2022. Radical production with pulsed beams: understanding the transition to FLASH. Int. J. Mol. Sci. 23, 13484 (Accepted).

Esplen, N., Mendonca, M.S., Bazalova-Carter, M., 2020. Physics and biology of ultrahigh dose-rate (FLASH) radiotherapy: a topical review. Phys. Med. Biol. 65 (23), 23TR03.

Favaudon, V., Caplier, L., Monceau, V., Pouzoulet, F., Sayarath, M., Fouillade, C., Poupon, M.-F., Brito, I., Hupé, P., Bourhis, J., 2014. Ultrahigh dose-rate FLASH irradiation increases the differential response between normal and tumor tissue in mice. Sci. Transl. Med. 6 (245), 245–293.

Felici, G., Barca, P., Barone, S., Bortoli, E., Borgheresi, R., De Stefano, S., Di Francesco, M., Grasso, L., Linsalata, S., Marfisi, D., 2020. Transforming an IORT linac into a FLASH research machine: procedure and dosimetric characterization. Front. Phys. 374.

Fouillade, C., Curras-Alonso, S., Giuranno, L., Quelennec, E., Heinrich, S., Bonnet-Boissinot, S., Beddok, A., Leboucher, S., Karakurt, H.U., Bohec, M., 2020. FLASH irradiation spares lung progenitor cells and limits the incidence of radio-induced senescence. Clin. Cancer Res. 26 (6), 1497–1506.

Friedl, A.A., Prise, K.M., Butterworth, K.T., Montay-Gruel, P., Favaudon, V., 2022. Radiobiology of the FLASH effect. Med. Phys. 49 (3), 1993–2013.

Ghita, M., Brown, K.H., Kelada, O.J., Graves, E.E., Butterworth, K.T., 2019. Integrating small animal irradiators with functional imaging for advanced preclinical radiotherapy research. Cancers 11 (2), 170.

Hewson, E., Butson, M., Hill, R., 2018. Evaluating TOPAS for the calculation of backscatter factors for low energy x-ray beams. Phys. Med. Biol. 63 (19), 195014.

Kuess, P., Bozsaky, E., Hopfgartner, J., Seifritz, G., Dörr, W., Georg, D., 2014. Dosimetric challenges of small animal irradiation with a commercial X-ray unit. Z. Med. Phys. 24 (4), 363–372.

Labarbe, R., Hotoiu, L., Barbier, J., Favaudon, V., 2020. A physicochemical model of reaction kinetics supports peroxyl radical recombination as the main determinant of the FLASH effect. Radiother. Oncol. 153, 303–310.

Lempart, M., Blad, B., Adrian, G., Bäck, S., Knöös, T., Ceberg, C., Petersson, K., 2019. Modifying a clinical linear accelerator for delivery of ultra-high dose rate irradiation. Radiother. Oncol. 139, 40–45.

Lu, G., Marsh, S., Damet, J., Carbonez, P., Laban, J., Bateman, C., Butler, A., Butler, P., 2017. Dosimetry in MARS spectral CT: TOPAS Monte Carlo simulations and ion chamber measurements. Australas. Phys. Eng. Sci. Med. 40 (2), 297–303.

Mazal, A., Prezado, Y., Ares, C., de Marzi, L., Patriarca, A., Miralbell, R., Favaudon, V., 2020. FLASH and minibeams in radiation therapy: the effect of microstructures on time and space and their potential application to protontherapy. Br. J. Radiol. 93 (1107), 20190807.

Micke, A., Lewis, D.F., Yu, X., 2011. Multichannel film dosimetry with nonuniformity correction. Med. Phys. 38 (5), 2523–2534.

Montay-Gruel, P., Bouchet, A., Jaccard, M., Patin, D., Serduc, R., Aim, W., Petersson, K., Petit, B., Bailat, C., Bourhis, J., 2018. X-rays can trigger the FLASH effect: ultra-high dose-rate synchrotron light source prevents normal brain injury after whole brain irradiation in mice. Radiother. Oncol. 129 (3), 582–588.

Montay-Gruel, P., Acharya, M.M., Petersson, K., Alikhani, L., Yakkala, C., Allen, B.D., Ollivier, J., Petit, B., Jorge, P.G., Syage, A.R., 2019. Long-term neurocognitive benefits of FLASH radiotherapy driven by reduced reactive oxygen species. Proc. Natl. Acad. Sci. USA 116 (22), 10943–10951.

Niroomand-Rad, A., Blackwell, C.R., Coursey, B.M., Gall, K.P., Galvin, J.M., McLaughlin, W.L., Meigooni, A.S., Nath, R., Rodgers, J.E., Soares, C.G., 1998. Radiochromic film dosimetry: recommendations of AAPM radiation therapy committee task group 55. Med. Phys. 25 (11), 2093–2115.

Perl, J., Shin, J., Schümann, J., Faddegon, B., Paganetti, H., 2012. TOPAS: an innovative proton Monte Carlo platform for research and clinical applications. Med. Phys. 39 (11), 6818–6837.

Rahman, M., Ashraf, M.R., Zhang, R., Bruza, P., Dexter, C.A., Thompson, L., Cao, X., Williams, B.B., Hoopes, P.J., Pogue, B.W., 2021. Electron FLASH delivery at treatment room isocenter for efficient reversible conversion of a clinical LINAC. Int. J. Radiat. Oncol. Biol. Phys. 110 (3), 872–882.

Rezaee, M., Iordachita, I., Wong, J.W., 2021. Ultrahigh dose-rate (FLASH) x-ray irradiator for pre-clinical laboratory research. Phys. Med. Biol. 66 (9), 095006.

Sanchez-Parcerisa, D., Sanz-García, I., Ibáñez, P., España, S., Espinosa, A., Gutiérrez-Neira, C., López, A., Vera, J.A., Mazal, A., Fraile, L.M., 2021. Radiochromic film dosimetry for protons up to 10 MeV with EBT2, EBT3 and unlaminated EBT3 films. Phys. Med. Biol. 66 (11), 115006.

Schüler, E., Trovati, S., King, G., Lartey, F., Rafat, M., Villegas, M., Praxel, A.J., Loo Jr., B. W., Maxim, P.G., 2017. Experimental platform for ultra-high dose rate FLASH irradiation of small animals using a clinical linear accelerator. Int. J. Radiat. Oncol. Biol. Phys. 97 (1), 195–203.

SEDECAL webpage. https://www.sedecal.com. Last access November 2022.

Senda, S., Sakai, Y., Mizuta, Y., Kita, S., Okuyama, F., 2004. Super-miniature x-ray tube. Appl. Phys. Lett. 85 (23), 5679–5681.

Sotiropoulos, M., Brisebard, E., Le Dudal, M., Jouvion, G., Juchaux, M., Crépin, D., Sebrie, C., Jourdain, L., Labiod, D., Lamirault, C., 2021. X-rays minibeam radiation therapy at a conventional irradiator: pilot evaluation in F98-glioma bearing rats and dose calculations in a human phantom. Clinic. Translation. Radiat. Oncol. 27, 44–49.

Syme, A., Kirkby, C., Mirzayans, R., MacKenzie, M., Field, C., Fallone, B., 2009. Relative biological damage and electron fluence in and out of a 6 MV photon field. Phys. Med. Biol. 54 (21), 6623.

Toshiba E7252X PI. https://etd.canon/en/product/pdf/xray/PE-E7252X_FX_GX_2018-11.pdf. Last access November 2022.

Toshiba E7869X PI. http://www.skphotoray.co.kr/datasheet/XRAYTUBE_E7869X.pdf. Last access November 2022.

Verhaegen, F., Nahum, A., Van De Putte, S., Namito, Y., 1999. Monte Carlo modelling of radiotherapy kV x-ray units. Phys. Med. Biol. 44 (7), 1767.

Verhaegen, F., Granton, P., Tryggestad, E., 2011. Small animal radiotherapy research platforms. Phys. Med. Biol. 56 (12), R55.

Vozenin, M.C., De Fornel, P., Petersson, K., Favaudon, V., Jaccard, M., Germond, J.-F., Petit, B., Burki, M., Ferrand, G., Patin, D., 2019. The advantage of FLASH radiotherapy confirmed in mini-pig and cat-cancer patients. Clin. Cancer Res. 25 (1), 35–42.

Vozenin, M.-C., Montay-Gruel, P., Limoli, C., Germond, J.-F., 2020. All irradiations that are ultra-high dose rate may not be FLASH: the critical importance of beam parameter characterization and in vivo validation of the FLASH effect. Radiat. Res. 194 (6), 571–572.

Wilson, J.D., Hammond, E.M., Higgins, G.S., Petersson, K., 2020. Ultra-high dose rate (FLASH) radiotherapy: silver bullet or fool's gold? Front. Oncol. 1563.

Yoshizumi, T., Brady, S.L., Robbins, M.E., Bourland, J.D., 2011. Specific issues in small animal dosimetry and irradiator calibration. Int. J. Radiat. Biol. 87 (10), 1001–1010.

Zhang, Q., Cascio, E., Li, C., Yang, Q., Gerweck, L.E., Huang, P., Gottschalk, B., Flanz, J., Schuemann, J., 2020. Flash investigations using protons: design of delivery system, preclinical setup and confirmation of flash effect with protons in animal systems. Radiat. Res. 194 (6), 656–664.